Available online at www.sciencedirect.com
SCIENCE DIRECT®
ELSEVIER
Journal of Magnetism and Magnetic Materials 293 (2005) 75–79
Journal of magnetism and magnetic materials
www.elsevier.com/locate/jmmm

Iron and Cobalt-based magnetic fluids produced by inert gas condensation

Nguyen H. Hai[a], Raymond Lemoine[a], Shaina Remboldt[a], Michelle Strand[a,d], Jeffrey E. Shield[b], David Schmitter[b], Robert H. Kraus, Jr. Michelle Espy[c], Diandra L. Leslie-Pelecky[a,*]

[a]*Department of Physics and Astronomy, Center for Materials Research and Analysis, University of Nebraska, Lincoln, NE 68588-0111 USA*
[b]*Department of Mechanical Engineering, Center for Materials Research and Analysis, University of Nebraska, Lincoln, NE 68588-0656 USA*
[c]*Biophysics Group, Los Alamos National Laboratory, Los Alamos NM 87545, USA*
[d]*Pius X High School, Lincoln, NE 68510, USA*

Available online 3 March 2005

Abstract

Iron and cobalt nanoparticle fluids have been prepared by inert-gas condensation into an oil/surfactant mixture. Superparamagnetic iron fluids (mean particle size = 11.6 ± 0.4 nm) and ferromagnetic cobalt fluids (mean particle size = 51.6 ± 3.4 nm) produced by this technique are promising candidates for magnetic targeting and hyperthermia applications.
© 2005 Published by Elsevier B.V.

Keywords: Ferrofluids; Inert-gas condensation; Nanoparticles; Iron; Cobalt; Synthesis

Magnetic fluids are of great interest to the biomagnetics community due to the wide variety of applications, which include magnetic imaging, sorting, targeting, and hyperthermia [1,2]. Each application requires optimizing different magnetic properties, so the development of techniques that allow fabrication of magnetic fluids with a broad range of properties is critical. Magnetic nanoparticles may be fabricated separately and dispersed in a fluid, or synthesized within a fluid [1,3]. Chemical synthesis and mechanical grinding are common fabrication methods; however, chemical reactions limit the materials that can be made by that method, and mechanical grinding has the disadvantage of producing large particle-size distributions.

Inert-gas condensation [4,5] is a process in which an atomic vapor is ejected into an inert

*Corresponding author. Tel.: +1 402 472 9178; fax: +1 402 472 2879.
E-mail address: diandra2@unl.edu (D.L. Leslie-Pelecky).

0304-8853/$ - see front matter © 2005 Published by Elsevier B.V.
doi:10.1016/j.jmmm.2005.01.046

gas (Ar, He or a mixture of both) at pressures $\sim 10^{-1}$ Torr. The vapor atoms thermalize via collisions with the inert gas, forming uniformly sized clusters. Clusters can be collected on a liquid-nitrogen-cooled rotating coldfinger and compacted to form a nanograined solid or deposited on a substrate with or without a matrix material [6]. Inert-gas condensed clusters can have mean sizes from 5–50 nm, with the mean size controlled by sputtering pressure, type of inert gas, gun-substrate distance, and sputtering power. Inert-gas condensation can be used to make clusters of virtually any material that can be vaporized by thermal evaporation, e-beam evaporation or sputtering, including ordered magnetic alloys [7,8] and oxides or nitrides using reactive sputtering [9]. This ultra-high-vacuum-based technique can produce 10–30 mg of magnetic clusters per hour.

Magnetic fluids, especially for in vivo applications, must have well-dispersed, separated clusters. Collecting clusters on a coldfinger can produce large agglomerates that do not disperse well in a fluid. Since many magnetic materials of interest oxidize when exposed to air, re-dispersal of inert-gas-condensed clusters in a fluid presents some challenges. Replacing the coldfinger by a drum rotating into a trough containing a fluid/surfactant mixture eliminates agglomeration and produces a well-dispersed magnetic fluid in a single step [9,10]. Fig. 1 shows a schematic illustration of inert-gas condensation into a fluid/surfactant mixture, with

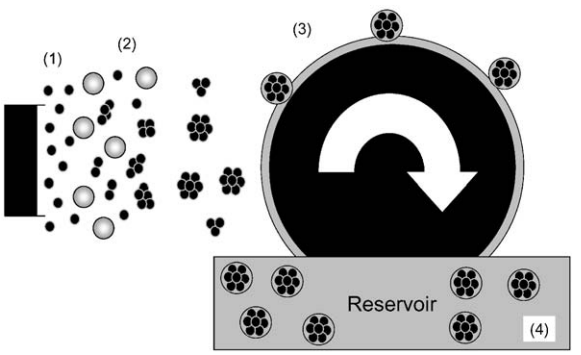

Fig. 1. Schematic illustration of the deposition process. Fe or Co vapor atoms (1) collide with inert-gas molecules (2). The resulting clusters are deposited on a rotating wheel (3) that is coated with a surfactant/oil mixture held in the reservoir (4).

the vapor atoms (1) colliding with inert-gas atoms to form clusters (2) that land on a fluid-coated drum (3) and are collected in a reservoir (4).

A turbomolecular or diffusion pump reduces the base pressure to $\sim 10^{-7}$ Torr, and controls the inert-gas pressure during deposition. The initial evacuation of the vacuum chamber degases the fluid/surfactant mixture. A shutter in front of the sputter source allows pre-sputtering of the target to remove any oxides on the target surface prior to deposition. Octoil® (vapor pressure $= 10^{-7}$ Torr) or Octoil-S® (vapor pressure $= 10^{-8}$ Torr) diffusion-pump oil is introduced using a load-lock system that allows transfer to and from the chamber without breaking vacuum or exposing the fluid to air. After sputtering, the fluid is decanted under vacuum into a flask and transferred into an argon-filled glovebox.

Iron and cobalt fluids were fabricated using pressed-powder, sintered sputtering targets made from 99.9% pure Fe or Co powder. The surfactants studied span a range of HLB (hydrophilic-lipophilic balance) values and include Hamposyl-O, Brij-92, Span 60, and Span 20 at concentrations from 1 to 30 vol%. Magnetic measurements were made using a SQUID susceptometer and an alternating gradient force magnetometer. Fluids were sealed in polyethylene bags for measurement.

As-made fluids are extremely stable for long periods of time. Particles can be separated from the fluid by acetone-induced flocculation, followed by high-speed centrifugation. The isolated particles can be re-dispersed in other carrier liquids. Fig. 2 shows a TEM micrograph of Fe nanoparticles in a mixture of 90 vol% Octoil® + 10 vol% Brij-92. The particles are spherical and 15–20 nm in diameter with a fairly small size distribution. Some agglomeration is evident, which likely is due to the washing process required to remove the particles from the oil. Electron diffraction indicates that the particles are single crystal.

The surfactants studied thus far do not provide adequate protection from oxidation, although such protection has been obtained in fluids made using other fabrication methods [11]. The magnetization of Fe fluids exposed to air for 15 min and then stored under argon is approximately the same as that of fluids that have not been exposed to air;

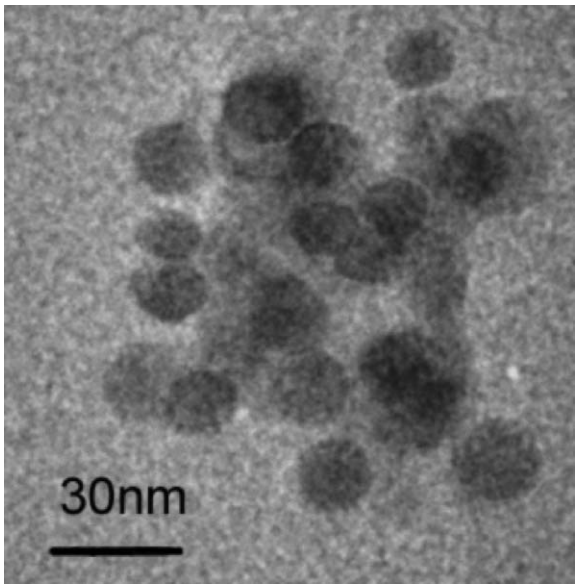

Fig. 2. TEM micrograph of Fe particles made in 90 vol% Octoil/10 vol% Brij-92.

however, leaving an iron fluid exposed to air for 24 h changes the fluid from a golden to a dark brown color. All samples discussed in this paper were stored, handled, and measured in an argon atmosphere to minimize oxidation.

Fig. 3 shows the magnetization as a function of field for an iron fluid at room temperature. Hysteresis loops for all samples show a superposition of a diamagnetic background and a ferro- or superpara-magnetic signal (as shown in trace 'a' of Fig. 3). The diamagnetism is attributed to the oil/surfactant mixture and has been subtracted in the hysteresis loops shown here. Magnetization is measured in emu/g total sample (i.e. magnetic particles + fluid).

Iron fluids with particles size of 15–20 nm are superparamagnetic at room temperature, with saturation occurring at much higher fields than in bulk iron—approximately 10 kOe at room temperature and 50 kOe at 10 K. The fluids become weakly ferromagnetic as the temperature decreases, with a coercivity of ~10 Oe at 10 K. Co fluids with 50-nm particle sizes are ferromagnetic at room temperature and show little change in the hysteretic properties between room temperature

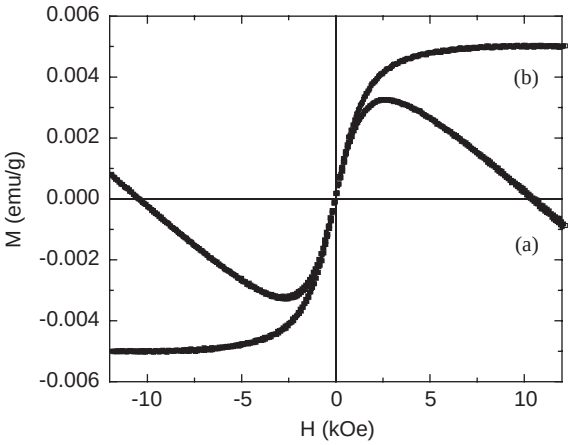

Fig. 3. $M(H)$ for an iron fluid, measured at room temperature. Curve 'a' is the raw data, and curve 'b' is the magnetization after a diamagnetic contribution has been removed.

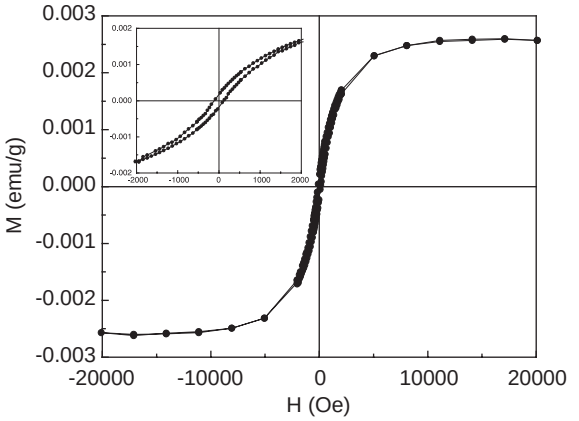

Fig. 4. $M(H)$ for a fluid with 50-nm cobalt nanoparticles at 100 K. The inset shows and expanded view of the low-field magnetization.

and 100 K. The primary change is a small increase in the low-field slope as the temperature decreases. Fig. 4 shows $M(H)$ at 100 K for a Co fluid, with the inset showing an expanded view of the low-field behavior. As with the Fe fluid, a much higher field is required to saturate the magnetization than is required for bulk Co. The coercivity is approximately 80 Oe and does not change significantly between room temperature and 100 K.

Fig. 5a shows the magnetization as a function of temperature for an iron fluid measured in two

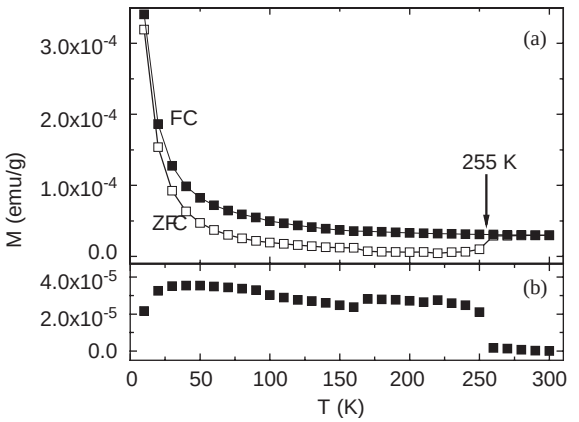

Fig. 5. (a) Field-cooled (M_{FC}, solid symbols) and zero-field-cooled (M_{ZFC} open symbols) magnetizations of iron fluid vs. temperature at 100 Oe. (b) $M_{FC} - M_{ZFC}$ vs. temperature. Error bars are smaller than the symbol size.

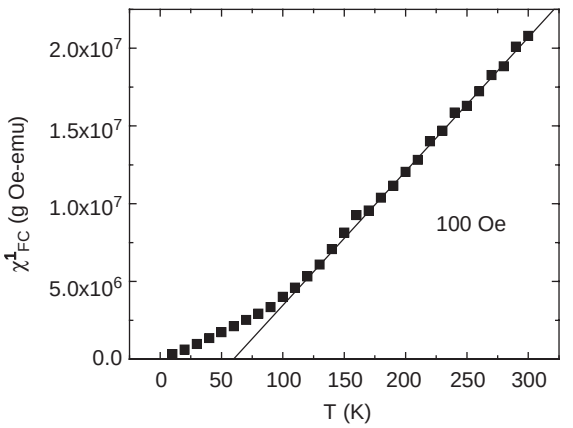

Fig. 6. The inverse susceptibility of the iron fluid as a function of temperature after subtracting a constant value. The resulting straight line has a temperature intercept of 61 ± 2 K.

different configurations. M_{ZFC} is the zero-field-cooled (ZFC) magnetization, in which the sample is cooled from room temperature to 5 K with no applied field, and is then measured in a field of 100 Oe as the temperature is increased. The field-cooled (FC) magnetization M_{FC} is obtained by cooling the sample in a 100-Oe field and then following the same measuring procedure. The offset between M_{ZFC} and M_{FC} is due to the liquefaction of the oil near 255 K. Fig. 5b shows the difference between the FC and ZFC magnetizations ($M_{FC} - M_{ZFC}$), which eliminates contributions from the reversible magnetization. The difference curve reveals a small jump near 150 K and a broad peak at lower temperatures.

This behavior is further elucidated by subtracting a constant——the value of $M(T = 300\,\mathrm{K})$—and plotting the inverse of the remaining FC susceptibility χ_{FC} as shown in Fig. 6. The feature at 150 K is present, but small. Fitting the inverse susceptibility to a Curie-Weiss form ($\chi_{FC} = C/(T - \theta)$, where C includes the supermoment) yields a Curie–Weiss temperature $\theta = 61 \pm 2$ K, indicating that the magnetic interactions are primarily ferromagnetic.

The dependence of the magnetization on the field cannot be described by a single Langevin equation, as shown by the dashed line of Fig. 7. Instead, the shape of the hysteresis loop is more

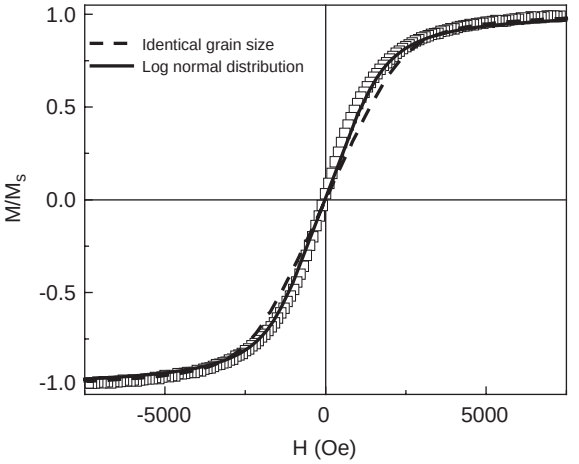

Fig. 7. Fit of $M(H)$ at room temperature of a Fe-based fluid to a single Langevin function (dashed line) and a distribution of Langevin functions as described by Eqs. (1) and (2).

closely approximated by fitting to an integral over a lognormal distribution of particle sizes.

$$M(H) = \int f(D)\, L(D, H)\, \mathrm{d}D, \tag{1}$$

where

$$f(D) = \frac{1}{\sqrt{2\pi}\sigma D}\, \mathrm{e}^{-((\ln(D_o) - \ln(D))^2/2\sigma^2)} \tag{2}$$

is the log-normal distribution usually found in particles made by inert-gas condensation, and $L(x)$

is the Langevin function $L(x) = \coth(x) - (1/x)$. The magnetization is assumed to scale with the volume of the magnetic particle. The fit to Eq. (1), shown as a solid line in Fig. 7, indicates a mean particle size $D_o = 11.6 \pm 0.4$ nm and a distribution breadth $\sigma = 2.2 \pm 0.1\,nm$. The mean diameter from the fit is slightly less than that determined from TEM images (~15 nm), but the small distribution breadth is consistent with the TEM results. The distribution of the Langevin functions is definitely a better fit than a single Langevin, but small deviations from the data remain. The lack of exact agreement may be due to a non-log-normal size distribution, or to inter-particle interactions.

The blocking temperature for 11.6-nm Fe particles (assuming the bulk value for the anisotropy constant of Fe of $4.8 \times 10^4\,J/m^3$), is about 100 K, while Fe particles with a diameter of 15 nm (as observed from TEM) would have a blocking temperature near 140 K. Anisotropy values can vary significantly in nanoparticles compared to the bulk, so it is difficult to assign meaning to either the feature near 50 K or the feature at 150 K based on this evidence.

In conclusion, we have produced Fe and Co magnetic fluids with narrow size distributions by inert-gas condensation directly into a fluid/surfactant mixture. Fe fluids with mean particle sizes on the order of 10–15 nm are superparamagnetic at room temperature, while Co fluids with 50-nm particles are ferromagnetic at room temperature. The inverse susceptibility of iron fluids deviates from a Curie–Weiss law near 50 K, suggesting the onset of interactions. Additional surfactants are being investigated to improve oxidation resistance and control particle size. Inert-gas condensation into fluids is a highly flexible technique with great potential for making different types of magnetic fluids with properties that can be tailored to address biomedical needs.

This project was supported by the Nebraska Research Initiative and the MRSEC program of the National Science Foundation (DMR-0213808). We thank V. Labhasetwar and T. Jain for assistance in surfactant selection.

References

[1] R.E. Rosenzweig, Ferrohydrodynamics, Cambridge University Press, Cambridge, 1985.
[2] U. Häfeli, W. Schütt, J. Teller, et al., Scientific and Clinical Applications of Magnetic Carriers, Plenum Press, New York, 1997.
[3] D.L. Leslie-Pelecky, R.D. Rieke, Chem. Mater. 8 (1996) 1770.
[4] H. Hahn, R. Averback, J. Appl. Phys. 67 (1990) 1113.
[5] C.G. Granqvist, R.A. Buhrman, J. Appl. Phys. 47 (1976) 220.
[6] H. Haberland, M. Karrais, M. Mall, et al., J. Vac. Sci. Technol. A 10 (1992) 3266.
[7] S. Stoyanov, V. Skumryev, Y. Zhang, et al., J. Appl. Phys. 93 (2003) 7592.
[8] S. Stoyanov, Y. Huang, Y. Zhang, et al., J. Appl. Phys. 93 (2003) 7190.
[9] I. Nakatani, T. Furubayashi, J. Magn. Magn. Mater. 85 (1990) 11.
[10] M. Wagener, B. Günther, J. Magn. Magn. Mater. 201 (1999) 41.
[11] M. Wagener, B. Günther, E. Blums, J. Magn. Magn. Mater. 201 (1999) 18.